ELSEVIER

Materials Science and Engineering A347 (2003) 265–279

MATERIALS SCIENCE & ENGINEERING A

www.elsevier.com/locate/msea

Particle dissolution and cross-diffusion in multi-component alloys

F.J. Vermolen [a,*], C. Vuik [a], S. van der Zwaag [b,c]

[a] *Department of Applied Mathematical Analysis, Delft University of Technology, Mekelweg 4, 2628 CD Delft, The Netherlands*
[b] *Laboratory of Materials Science, Delft University of Technology, Rotterdamse weg 137, 2628 AL Delft, The Netherlands*
[c] *Netherlands Institute for Metals Research (N.I.M.R.), Rotterdamse weg 137, 2628 AL Delft, The Netherlands*

Received 26 April 2002; received in revised form 31 July 2002

Abstract

A general model for the dissolution of stoichiometric particles, taking into account the influences of cross-diffusion, in multi-component alloys is proposed and analyzed using a diagonalization argument. It is shown that particle dissolution in multi-component alloys with cross-diffusion can under certain circumstances be approximated by a model for particle dissolution in binary alloys. Subsequently, the influence of cross-diffusion on particle dissolution rate is analyzed for planar and spherical particles. Further, we show some numerical simulations and conclude that cross-diffusion can be incorporated into multi-component dissolution models.

Keywords: Multi-component alloy; Particle dissolution; Cross-diffusion; Vector-valued Stefan problem; Self-similar solution

1. Introduction

In the thermal processing of both ferrous and non-ferrous alloys, homogenization of the as-cast microstructure by annealing at such a high temperature that unwanted precipitates are fully dissolved, is required to obtain a microstructure suited to undergo heavy plastic deformation. Such a homogenization treatment, to name just a few examples, is applied in hot-rolling of Al killed construction steels, HSLA steels, all engineering steels, as well as aluminium extrusion alloys. Although precipitate dissolution is not the only metallurgical process taking place, it is often the most critical of the occurring processes. The minimum temperature at which the annealing should take place can be determined from thermodynamic analysis of the phases present. Another important quantity is the minimum annealing time at this temperature. This time, however, is not a constant but depends on particle size, particle geometry, particle concentration, overall composition etc.

Due to the scientific and industrial relevance of being able to predict the kinetics of particle dissolution, many models of various complexity have been presented and experimentally validated. The early models on particle dissolution based on long-distance diffusion were based on analytical solutions in an unbounded medium under the assumption of local equilibrium at the moving interface, see Whelan [1] for instance. The model of Nolfi et al. [2] incorporate the interfacial reaction between the dissolving particle and its surrounding phase. Later modeling particle dissolution has been extended to the introduction of multi-component particles by, among others, Reiso et al. [3], Hubert [4]. All the above mentioned models were based on viewing particle dissolution as a Stefan problem. A recent approach is the phase-field approach, which is derived from a minimization of the energy functional. This approach has, among others, been used by Kobayashi [5] to simulate dendritic growth. A recent extension to multi-component phase-field computation is done by Grafe et al. [6], where solidification and solid state transformations are modeled. For the one-dimensional case they obtain a perfect agreement between the phase-field approach and the software package DICTRA which is based on a sharp interface between constituent phases. Some disadvantages of the phase-field approach are that

* Corresponding author. Tel.: +31-15-278-1833; fax: +31-15-278-7209.
E-mail address: f.j.vermolen@its.tudelft.nl (F.J. Vermolen).

0921-5093/02/$ - see front matter
PII: S0921-5093(02)00615-9

(1) no simple quick estimates of the solution are available and (2) physically justifiable parameter values in the energy functional are not easy to obtain: generally these quantities are to be obtained by using fitting procedures that link experiment and numerical computation. Therefore, we limit ourselves in the present work to model particle dissolution as a Stefan problem, where a multi-component 'generalized' Fick diffusion equation including cross-diffusion coefficients has to be solved with a moving interface separating the constituent solute and solvent phases.

Kale et al. [7] consider ternary diffusion in FCC phases of Fe–Ni–Cr alloy systems. They compute diffusion coefficients, including cross-diffusion coefficients, by using the thermodynamically based Boltzmann–Matano method. In their metallic systems the cross-diffusion coefficients range in value up to about a third of those of the diagonal diffusion coefficients. Hence cross-diffusion should be taken into account here. Vergara et al. [8] recently emphasized the significance of cross-terms in the 'generalized' Fick diffusion equation. They construct a model to evaluate (cross) diffusion coefficients from experiments. They apply their model to a reference system containing Sodiumchloride in water, Travis and Gubbins [9] compute cross-diffusion coefficients in graphite slit pores using Monte-Carlo simulations. The formalism of cross-diffusion in multi-component metallic alloys has been motivated in terms of chemical potentials by Kirkaldy and Young [10]. In their work, an analytical solution of the obtained system of diffusion equations has been given for a one-dimensional and unbounded geometry. They note that the eigenvalues of the diffusion matrix have to be real-valued and positive for an acceptable physical problem. A more recent book where cross-diffusion is also treated is the book of Glicksman [11]. Here a self-similar solution of the equations is given where the boundaries are fixed. A numerical solution of the diffusion equations for fixed boundaries including cross-diffusion was recently obtained by Naumann and Savoca [12].

As far as we know, no extension to problems that incorporate the movement of the interface has been made yet. It is the aim of this work to analyze the combination of a moving boundary with cross-diffusion effects. Existence of (multiple) solutions when the diffusion matrix is singular is stated and proven as mathematical theorems in [13]. In the present study, we give asymptotic solutions for the dissolution of a planar and spherical particle. Furthermore, we show that under certain circumstances the multi-component problem with cross-diffusion terms (a strongly coupled 'vector-valued' Stefan problem) can be approximated by a binary problem ('scalar' Stefan problem). Subsequently we present a numerical method that is used to solve the Stefan problem and give some numerical results for hypothetical alloys. Finally some conclusions are presented.

We remark that this study is an extension of earlier work described in [14–16] where influences of cross-diffusion on the dissolution problem were not incorporated yet.

2. Basic assumptions in the model

The as-cast microstructure is simplified into a representative cell containing the 'matrix' of phase α and a single particle of phase β of a specific form, size and location of the cell boundary. To avoid confusion we use the notation 'matrix' for a phase surrounding the dissolving particle and the notation matrix to indicate the mathematical notion of a two-dimensional array of numbers.

Both a uniform and a spatially varying initial composition at $t = 0$ can be assumed in the model. The boundary between the β-particle and α-'matrix' is referred to as the interface. Particle dissolution is assumed to proceed by a number of the subsequent steps [2]: decomposition of the particle, atoms from the particle crossing the interface and diffusion of these atoms in(to) the α-phase. Here we take the effects of cross-diffusion into account. We assume in this work that the first two mechanisms proceed sufficiently fast with respect to diffusion. Hence, the interfacial concentrations are those as predicted by thermodynamics (local equilibrium).

In [15], we considered the dissolution of a stoichiometric particle in a ternary and a general multi-component alloy. We denote the chemical species by Sp_i, $i \in \{1, \ldots, n+1\}$, where Sp_{n+1} is the 'original' solvent metallic α-phase in which the particle dissolves. We denote the stoichiometry of the particle by $(\mathrm{Sp}_1)_{m_1}(\mathrm{Sp}_2)_{m_2}(\mathrm{Sp}_3)_{m_3}(\ldots)(\mathrm{Sp}_n)_{m_n}$. The numbers m_1, m_2, …, m_n are stoichiometric constants. We denote the interfacial concentration of species i by c_i^{sol} and we use the following hyperbolic relationship for the interfacial concentrations:

$$(c_1^{\mathrm{sol}})^{m_1}(c_2^{\mathrm{sol}})^{m_2}(\ldots)(c_n^{\mathrm{sol}})^{m_n} = K. \tag{1}$$

The factor K is referred to as the solubility product. It depends on temperature T according to an Arrhenius relationship, in the present work, however, we assume it to be constant.

We denote the position of the moving interface between the β-particle and α-phase by $S(t)$, where t denotes time. Consider a one-dimensional domain, i.e. there is one spatial variable, which extends from 0 up to M (the cell size). Since particles dissolve simultaneously in the metal, the concentration profiles between consecutive particles may interact and hence soft-impingement occurs. This motivates the introduction of a

finitely sized cell over whose boundary there is no flux. For cases of low overall concentrations in the alloy, the cell size M may be large and the solution resembles the case where M is infinite. The spatial co-ordinate is denoted by r, $0 \leq S(t) \leq r \leq M$. This domain is referred to as $\Omega(t) := \{r \in \mathbb{R}: S(t) \leq r \leq M\}$. The α-'matrix', where diffusion takes place, is given by $\Omega(t)$ and the β-particle is represented by the domain $0 \leq r \leq S(t)$. Keeping cross-diffusion in mind, we have for each alloying element, with $r \in \Omega(t)$ and $t > 0$:

$$\frac{\partial c_i}{\partial t} = \sum_{j=1}^{n} \frac{1}{r^a} \frac{\partial}{\partial r} \left\{ D_{ij} r^a \frac{\partial c_j}{\partial r} \right\}, \quad \text{for } i \in \{1, \ldots, n\}. \tag{2}$$

The geometry is planar, cylindrical and spherical for, respectively, $a = 0$, 1 and 2. The above equations follow from thermodynamic considerations, their derivation can for instance be found in [10]. Here D_{ij} and c_i, respectively, denote the coefficients of the diffusion matrix and the concentration of the species i in the α-rich phase. The diffusion matrix D is notated as follows:

$$D = \begin{pmatrix} D_{11} & \ldots & D_{1n} \\ \ldots & \ldots & \ldots \\ D_{n1} & \ldots & D_{nm} \end{pmatrix}. \tag{3}$$

The off-diagonal entries of D (i.e. D_{ij}, $i \neq j$), also referred to as the cross-terms, are a measure for the interaction of diffusion in the 'matrix; between consecutive alloying elements. When an alloying element is dissolved in the α-'matrix' then the resulting stress and elongations in the crystal structure facilitate or worsen diffusion of the other elements. The off-diagonal entries of D are a measure of for this mutual influence. When $D_{ij} < 0$, then alloying element j deteriorates diffusion of element i in the α-'matrix', whereas $D_{ij} > 0$ implies that element j facilitates diffusion of element i in the α-'matrix'. An alternative formulation of cross-diffusion is treated by Farkas [17] where only the diagonal entries of the above diffusion matrix are used, however, these diagonals are taken to depend on the concentration of all the other species and hence a strong coupling arises in a different way. We do not treat this approach in this study but we will use the formulation of Eq. (2) that has been motivated in [10]. We further assume that the diffusion matrix does not depend on the concentration, time and space, i.e. the matrix is treated as a constant in the present work. We note that the matrix D generally depends on time when the particle dissolves during a non-isothermal heat treatment.

Let c_i^0 denote the initial concentration of each element in the α-phase, then we take as initial conditions (IC):

$$\text{(IC)} \begin{cases} c_i(r, 0) = c_i^0(r) & \text{for } i \in \{1, \ldots, n\} \\ S(0) = S_0. \end{cases} \tag{4}$$

At a boundary not being an interface, i.e. at M or when $S(t) = 0$; we assume no flux through it, i.e.:

$$\sum_{j=1}^{n} D_{ij} \frac{\partial c_j}{\partial v} = 0, \quad \text{for } i \in \{1, \ldots, n\}. \tag{5}$$

Here v represents the outward normal vector of a cell. When D is not singular, then Eq. (5) holds if and only if:

$$\frac{\partial c_i}{\partial v} = 0, \quad \text{for } i \in \{1, \ldots, n\}. \tag{6}$$

Furthermore at the moving interface $S(t)$ we have the 'Dirichlet boundary condition' c_i^{sol} for each alloying element. The concentration of element i in the particle is denoted by c_i^{part}, this concentration is fixed at all stages. This assumption follows from the constraint that the stoichiometry of the particle is maintained during dissolution in line with Reiso et al. [3]. The dissolution rate (interfacial velocity) is obtained from a mass-balance of the atoms of alloying element i. The mass-balance per unit area leads to:

$$\frac{(S(t + \Delta t) - S(t))}{\Delta t} (c_i^{\text{part}} - c_i^{\text{sol}}) = \sum_{j=1}^{n} D_{ij} \frac{\partial c_j}{\partial r}(S(t), t). \tag{7}$$

Subsequently we take the limit $\Delta t \to 0$ and we obtain the following equation for the interfacial velocity:

$$(c_i^{\text{part}} - c_i^{\text{sol}}) \frac{\mathrm{d}S}{\mathrm{d}t} = \sum_{j=1}^{n} D_{ij} \frac{\partial c_j}{\partial r}. \tag{8}$$

Summarized, we obtain at the interface for $t > 0$ and $i, j \in \{1, \ldots, n\}$:

$$\left.\begin{aligned} & c_i(S(t), t) = c_i^{\text{sol}} \\ & (c_i^{\text{part}} - c_i^{\text{sol}}) \frac{\mathrm{d}S}{\mathrm{d}t} = \sum_{j=1}^{n} D_{ij} \frac{\partial c_j}{\partial r}(S(t), t) \end{aligned}\right\}$$

$$\Rightarrow \sum_{k=1}^{n} \frac{D_{ik}}{c_i^{\text{part}} - c_i^{\text{sol}}} \frac{\partial c_k}{\partial r}(S(t), t) = \sum_{k=1}^{n} \frac{D_{jk}}{c_j^{\text{part}} - c_j^{\text{sol}}} \frac{\partial c_k}{\partial r}(S(t), t) \tag{9}$$

The right-hand side of above equations follows from local mass-conservation of the components. Above formulated problem falls within the class of Stefan-problems, i.e. diffusion with a moving boundary. Since we consider simultaneous diffusion of several chemical elements, it is referred to as a 'vector-valued Stefan problem'. The unknowns in above equations are the concentrations c_i, interfacial concentrations c_i^{sol} and the interfacial position $S(t)$, All concentrations are by necessity non-negative. The coupling exists in both the diffusion equations, Stefan condition and the values of the concentrations at the interfaces between the particle

and α-rich phase. This strong coupling complicates the qualitative analysis of the equations. For a mathematical overview of Stefan problems we refer to the textbooks of Crank [18], Chadarn and Rasnmssen [19] and Visintin [20].

3. Analysis

In this section, we factorize the diffusion matrix by use of its eigenvalues and (generalized) eigenvectors according to standard linear algebra procedures. This is done to facilitate the mathematical problem that has to he solved. A direct consequence of the factorization is that the cross-terms in the equations vanish and the diffusion coefficients are replaced by the eigenvalues of the diffusion matrix. In most cases the diffusion matrix is diagonalizable and the strong coupling vanishes between the diffusion equations. However, when the diffusion matrix is not diagonalizable then some or one diffusion equation is uncoupled whereas the rest of the diffusion equations are coupled. Further, the solution of the transformed diffusion equations in general no longer satisfies a maximum principle and hence extremes away from the boundaries may be present also for $t>0$ when the diffusion matrix is not diagonalizable. We refer to [13] for a more extensive treatment. The analytical solutions that we present here are based on self-similarity and for an unbounded domain.

3.1. Decomposition of the diffusion matrix

First we write the equations in a vector-notation and we define the vectors $\underline{c}:=(c_1,\ c_2,\ \ldots,\ c_n)^{\mathrm{T}}$, $\underline{c}^{\mathrm{p}}:=(c_1^{\mathrm{part}},\ c_2^{\mathrm{part}},\ \ldots,\ c_n^{\mathrm{part}})^{\mathrm{T}}$ and $\underline{c}^{\mathrm{s}}:=(c_1^{\mathrm{sol}},\ c_2^{\mathrm{sol}},\ \ldots,\ c_n^{\mathrm{sol}})^{\mathrm{T}}$, then the diffusion equations can be written as:

$$\frac{\partial}{\partial t}\ \underline{c}=\frac{1}{r^a}\frac{\partial}{\partial r}\left\{r^a D\frac{\partial}{\partial r}\right\}\underline{c}. \tag{10}$$

The boundary and IC follow similarly in vector notation. The Stefan condition becomes in vector notation:

$$(\underline{c}^{\mathrm{p}}-\underline{c}^{\mathrm{s}})\frac{\mathrm{d}S}{\mathrm{d}t}=\frac{\partial}{\partial r}\ D\underline{c}(S(t),\ t). \tag{11}$$

We assume that the matrix D is diagonalizable. To analyze Eq. (11) we use the Decomposition Theorem, which can for instance be found in [21], page 317. The theorem says that for each real-valued $n\times n$-matrix D there exists a non-singular $n\times n$-matrix P such that:

$$D=P\Lambda P^{-1}, \tag{12}$$

where Λ is a diagonal matrix containing the eigenvalues of matrix D:

$$\Lambda=\begin{pmatrix}\lambda_1 & 0 & 0 & \ldots & 0 & \\ 0 & \lambda_2 & 0 & 0 & \ldots & 0\\ 0 & 0 & \lambda_3 & 0 & \ldots & \\ 0 & \ldots & \ldots & \ldots & \ldots & \lambda_n\end{pmatrix}. \tag{13}$$

In our case the set $\{\lambda_n\}$ correspond to the eigenvalues of the diffusion matrix D.

The matrix P has columns that are formed by the eigenvectors of D. The arrangement is in the same order as the set $\{\lambda_n\}$ in the matrix Λ, The eigenvalues and eigenvectors are obtained from:

$$\det(D-\lambda I)=0,\quad \text{giving } \{\lambda_1,\ \ldots,\ \lambda_n\} \tag{14}$$

$$D\underline{v}_i=\lambda_i\underline{v}_i, \tag{15}$$

note that some of the eigenvalues may be equal.

When the matrix D is not diagonalizable, we consider an eigenvalue λ_i of multiplicity p in Eq. (14). For this case, we have $\lambda_j=\lambda_i$ for $j\in\{i,\ \ldots,\ i+p\}$. The generalized eigenvectors that are substituted into the columns of P are obtained from:

$$D\underline{v}_i=\lambda_i\underline{v}_i, \tag{16}$$

$$(D-\lambda_i I)\underline{v}_{j+1}=\underline{v}_j,\quad \text{for } j\in\{i,\ \ldots,\ i+p-1\}. \tag{17}$$

In the second equation above we assume that $\lambda_j=\lambda_i$ for all $j\in\{i,\ldots,i+p\}$ and that v_j depends linearly on its preceding eigenvectors. In Eq. (17), I is the $n\times n$-identity matrix. Further, Λ becomes a Jordan block matrix when D is not diagonalizable. We refer to [13] for a more extensive treatment of the case where D is not diagonalizable.

We remark that Kirkaldy et al. [22] use a thermodynamic argument to show that the eigenvalues of the diffusion matrix are positive and real-valued. Therefore, we limit ourselves to cases where the eigenvalues are real-valued and positive.

3.1.1. An example for a ternary alloy

We consider a ternary example, with the following real-valued matrix:

$$D=\begin{pmatrix}D_{11} & D_{12}\\ D_{21} & D_{22}\end{pmatrix}. \tag{18}$$

From Eq. (14) follows that the eigenvalues are determined from:

$$(D_{11}-\lambda)(D_{22}-\lambda)-D_{12}D_{21}=0\Leftrightarrow \tag{19}$$

$$\Leftrightarrow\lambda=\frac{D_{11}+D_{22}\pm\sqrt{(D_{11}+D_{22})^2-4(D_{11}D_{22}-D_{12}D_{21})}}{2} \tag{20}$$

We remark that when the trace of D is positive, $\mathrm{tr}(D):=D_{11}+D_{22}>0$, and:

$$\det(D) = D_{11}D_{22} - D_{12}D_{21} \in \left(0, \frac{\mathrm{tr}(D)^2}{4}\right), \tag{21}$$

then the eigenvalues of D are real and have a positive value.

3.2. Transformation of the diffusion equations

For the remaining text we assume that the eigenvalues of D are real and positive. Substitution of the decomposition of D, Eq. (12) into Eq. (11) gives:

$$\frac{\partial}{\partial t}\,\underline{c} = \frac{1}{r^a}\frac{\partial}{\partial r}\left\{r^a \frac{\partial}{\partial r}\right\} P\Lambda P^{-1}\underline{c} \Leftrightarrow \frac{\partial}{\partial t}\; P^{-1}\underline{c}$$
$$= \frac{1}{r^a}\frac{\partial}{\partial r}\left\{r^a \frac{\partial}{\partial r}\right\}\Lambda P^{-1}\underline{c}$$

$$(\underline{c}^{\mathrm{p}} - \underline{c}^{\mathrm{s}})\frac{\mathrm{d}S}{\mathrm{d}t} = \frac{\partial}{\partial r}\; P\Lambda P^{-1}\underline{c}(S(t),\ t) \Leftrightarrow P^{-1}(\underline{c}^{\mathrm{p}} - \underline{c}^{\mathrm{s}})\frac{\mathrm{d}S}{\mathrm{d}t}$$
$$= \frac{\partial}{\partial r}\; \Lambda P^{-1}\underline{c}(S(t),\ t). \tag{22}$$

We define the transformed concentrations as:

$$\underline{u} := P^{-1}\underline{c}, \qquad \underline{u}^{\mathrm{s}} := P^{-1}\underline{c}^{\mathrm{s}}, \qquad u^{\mathrm{p}} := P^{-1}\underline{c}^{\mathrm{p}},$$
$$\underline{u}^0 := P^{-1}\underline{c}^0. \tag{23}$$

Then the diffusion equation and equation of motion change into:

$$\frac{\partial}{\partial t}\underline{u} = \frac{1}{r^a}\frac{\partial}{\partial r}\left\{r^a \frac{\partial}{\partial r}\right\}\Lambda\underline{u} \tag{24}$$

$$(\underline{u}^{\mathrm{p}} - \underline{u}^{\mathrm{s}})\frac{\mathrm{d}S}{\mathrm{d}t} = \frac{\partial}{\partial r}\; \Lambda\underline{u}(S(t),\ t). \tag{25}$$

Note that the system given in Eq. (24) is fully uncoupled. The homogeneous Neumann conditions at the non-moving boundary are similar for the transformed concentrations. Further, we have for $t = 0$.

$$u_j = \begin{cases} u_j^0, & \text{for } r \in (S(0),\ M], \\ u_j^{\mathrm{part}}, & \text{for } r \in [0,\ S(0)]. \end{cases} \qquad j \in \{1,\ \ldots,\ n\} \tag{26}$$

From $\underline{c} = P\underline{u} \Rightarrow c_i = \Sigma_{j=1}^{n}\, p_{ij}u_j$, the coupling between the interfacial concentrations via the hyperbolic relation Eq. (1) changes into:

$$\left(\sum_{j=1}^{n} p_{1j}u_j^{\mathrm{s}}\right)^{m_1}\left(\sum_{j=1}^{n} p_{2j}u_j^{\mathrm{s}}\right)^{m_2}(\ldots)\left(\sum_{j=1}^{n} p_{nj}u_j^{\mathrm{s}}\right)^{m_n}$$
$$= K. \tag{27}$$

The analysis is facilitated using the diagonalization of the diffusion matrix. We see that the coupling between subsequent concentrations only remains in the above Eqs. (27) and (25).

4. Similarity solutions and asymptotic approximations

We consider analytical solutions satisfying Eq. (2) for the concentrations. We illustrate the importance of cross-diffusion in the above problem by the use of the exact self-similar solution for problem (P_1), which is derived in [13] for the planar case, where $a = 0$ in Eq. (24), Fig. 1 displays dissolution curves computed for various values of cross-diffusion coefficient D_{12} where we use the following data-set:

$$\underline{c}^0 = (0,\ 0)^{\mathrm{T}} \qquad \underline{c}^{\mathrm{part}} = (50,\ 50)^{\mathrm{T}}, \qquad D = \begin{pmatrix} 1 & D_{12} \\ D_{12} & 2 \end{pmatrix},$$
$$K = 1. \tag{28}$$

The above diffusion matrix is symmetric. From Fig. 1, it is clear that the influence of the cross-terms is significant. Since Kale et al. [7] indicate that the cross-diffusion terms can have the same order of magnitude as the diagonal terms in the diffusion matrix we choose the values of D_{12} in the range $[-1, 0]$.

We, however, will use the approximation by Aaron and Kotler [23] for the planar case and the approximation by Whelan [1] for the spherical case. Both approaches are derived with the use of Laplace transforms where the interfacial position is assumed to move far more slowly than the rate of diffusion in the α-'matrix'. This turns out to be a good approximation when $|u_i^{\mathrm{s}} - u_i^0| \ll |u_i^{\mathrm{p}} - u_i^{\mathrm{s}}|$. This is illustrated in some examples in the remainder of this section. With both approches an easy solvable problem arises for the estimation of the dissolution rate for a planar and spherical particle in a multi-component alloy with cross-diffusion. We will only discuss this for the case of a diagonalizable diffusion matrix. The case of a non-diagonalizable matrix is more complicated but can be treated analogously, see [13] for more details on the mathematics for the non-diagonalizable case. For the planar case, we give an estimate for the dissolution rate in terms of a quasi-binary formulation of the multi-component dissolution problem with cross-diffusion. Finally, we use the Whelan [1] approach to obtain a semi-analytical approach for the spherical case.

4.1. An asymptotic solution for the planar case

Suppose that $|u_i^{\mathrm{s}} - u_i^0| \ll |u_i^{\mathrm{p}} - u_i^{\mathrm{s}}|$ then Aaron and Kotler [23] give the following equation for interface motion for a given combination of u_i^{s}, u_i^{p} and u_i^0:

$$\frac{\mathrm{d}S}{\mathrm{d}t} = \frac{u_i^0 - u_i^{\mathrm{s}}}{u_i^{\mathrm{p}} - u_i^{\mathrm{s}}}\sqrt{\frac{\lambda_i}{\pi t}} =: \frac{k}{2\sqrt{t}}. \tag{29}$$

Since the solution for $\mathrm{d}S/\mathrm{d}t$ should be the same for all components i, this implies with combination with Eq. (27) that the solution of problem (P_1) is approximated

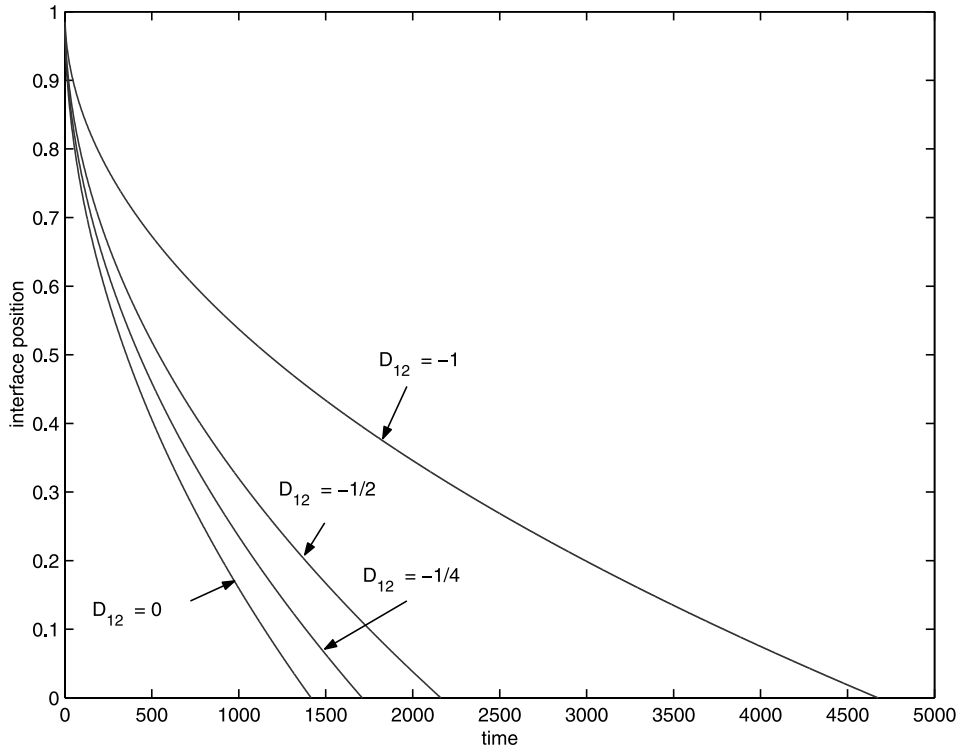

Fig. 1. The interface position as a function of time for the exact self similar solution for several values of the cross-diffusion terms.

by the solution for k and u_i^{s} of:

$$(P_1)\begin{cases} k = 2\dfrac{u_i^0 - u_i^{\mathrm{s}}}{u_i^{\mathrm{p}} - u_i^{\mathrm{s}}}\sqrt{\dfrac{\lambda i}{\pi}}, \quad \text{for } i \in \{1, \ldots, n\}, \\ \left(\displaystyle\sum_{j=1}^{n} p_{1j}u_j^{\mathrm{s}}\right)^{m_1}\left(\sum_{j=1}^{n} p_{2j}u_j^{\mathrm{s}}\right)^{m_2}(\ldots)\left(\sum_{j=1}^{n} p_{nj}u_j^{\mathrm{s}}\right)^{m_n} = K \end{cases}$$

The above problem follows from the approach due to Aaron and Kotler [23] and can be solved by using a, zero-point method. The derivation of this approach is based on the Laplace transform of the diffusion equation. The approach can also be derived from the exact self-similar solution, this is done in [13]. We continue on a simplification of the above problem to obtain an explicit solution. Suppose that the initial concentrations are zero, then $\underline{u}^0 = \underline{0}$ and hence that the transformed particle concentration is much larger than the transformed interfacial concentrations, i.e. $u_i^{\mathrm{s}} \ll u_i^{\mathrm{p}}$ for $i \in \{1, \ldots, n\}$ then the first equation of (P_1) with $i = 1$ becomes:

$$k \approx -2\frac{u_1^{\mathrm{s}}}{u_1^{\mathrm{p}}}\sqrt{\frac{\lambda_1}{\pi}}. \tag{30}$$

Hence the equation of motion of the interface becomes

$$\frac{\mathrm{d}S}{\mathrm{d}t} \approx -\frac{u_1^{\mathrm{s}}}{u_1^{\mathrm{p}}}\sqrt{\frac{\lambda_1}{\pi t}}. \tag{31}$$

Further, the following recurrence relation between the transformed interfacial concentrations follows:

$$u_i^{\mathrm{s}} = \frac{u_i^{\mathrm{p}}}{u_1^{\mathrm{p}}}\sqrt{\frac{\lambda_1}{\lambda_i}}\,u_1^{\mathrm{s}}. \tag{32}$$

Substitution of above transformed interfacial concentrations into the second equation of (P_2) gives the following real-valued solution:

$$u_1^{\mathrm{s}} = \left(\frac{K}{\left(\displaystyle\sum_{j=1}^{n} p_{1j}\frac{u_j^{\mathrm{p}}}{u_1^{\mathrm{p}}}\sqrt{\frac{\lambda_1}{\lambda_j}}\right)^{m_1}\left(\sum_{j=1}^{n} p_{2j}\frac{u_j^{\mathrm{p}}}{u_1^{\mathrm{p}}}\sqrt{\frac{\lambda_1}{\lambda_j}}\right)^{m_2}(\ldots)\left(\sum_{j=1}^{n} p_{nj}\frac{u_j^{\mathrm{p}}}{u_1^{\mathrm{p}}}\sqrt{\frac{\lambda_1}{\lambda_j}}\right)^{m_n}}\right)^{1/\mu}, \tag{33}$$

where we defined $\mu := \Sigma_{j=1}^{n} m_j$. Above expression for the transformed interfacial concentration is substituted into

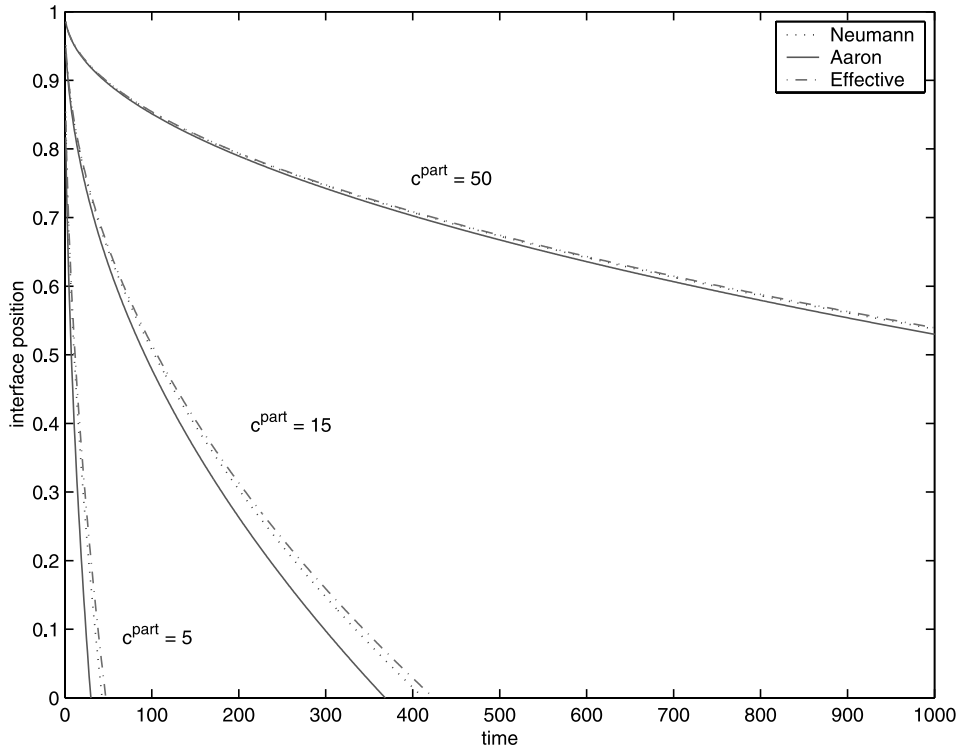

Fig. 2. The interface position as a function of time for the several approaches. The cross-diffusion coefficient $D_{12} = -1$, $K = 1$ and otherwise the same data set is used as in Fig. 1.

the rate equation for the interface (Eq. (30)). This gives:

$$\frac{\mathrm{d}S}{\mathrm{d}t} = -\frac{K^{1/\mu}}{u_1^p}\left[\prod_{k=1}^{n}\frac{1}{\left(\sum_{j=1}^{n}\left(p_{kj}\left(u_j^p/u_1^p\sqrt{\lambda_1/\lambda_j}\right)\right)\right)^{mk}}\right]^{1/\mu} \times\sqrt{\frac{\lambda_1}{\pi t}}. \tag{34}$$

The above equation is referred to as the quasi-binary approach or as the effective approximation. From the above equation dissolution times of the particle can be estimated easily using known parameters such as the eigenvalues and eigenvectors of the diffusion matrix. Furthermore, the solubilities obtained from the above equations can be used as initial guesses for the zero-point method to solve for the semi-explicit solution and numerical solutions.

In Fig. 2 we show the interface position, computed by the use of the exact 'Neumann' solution for the planar case (see [13]), (P_1) (the'Aaron' approximation) and Eq. (34) (the 'effective' approximation), as a function of time for $K = 1$ and $\underline{c}^{\mathrm{p}} = (50, 50)^{\mathrm{T}}$, $\underline{c}^{\mathrm{p}} = (15, 15)^{\mathrm{T}}$ and $\underline{c}^{\mathrm{p}} = (5, 5)^{\mathrm{T}}$. The other data are the same as in Fig. 1. It can be seen that for high particle concentrations $\underline{c}^{\mathrm{p}} = (50, 50)^{\mathrm{T}}$ the difference between all the approaches is small. Whereas for lower particle concentrations the difference increases significantly. The results of the case that $K =$ 50 with otherwise the same data are plotted in Fig. 3. For this case, the difference between the several approaches is larger. This is due to the fact that u_i^{s} becomes large with respect to the transformed particle concentration u_i^{p}.

To illustrate that the difference between the various approaches is hardly influenced by the value of the cross-diffusion coefficient we plot the dissolution time as a function of D_{12} in Fig. 4 with otherwise the same data as in Fig. 1. Until now, the approach by the use of Eq. (34) turned out to be an accurate approach for the computation of dissolution times. However, when the initial concentrations deviate from zero, as shown in Fig. 5, where otherwise the same data-set is used as in Fig. 1 with $D_{12} = -1$, the approach with Eq. (34) breaks down. Therefore, we conclude that the approach by solving (P_1) is robust. Its solution is a good approximation of the exact solution for the planar case. The quasi-binary approach from Eq. (34) is recommended for use only when the initial concentrations are very small. When this is fulfilled then the approach from Eq. (34) gives a quick qualitative insight into the dissolution kinetics.

4.2. An approximate solution for the spherical case

We apply the approximation due to Whelan in the computations for the dissolution of a spherical particle.

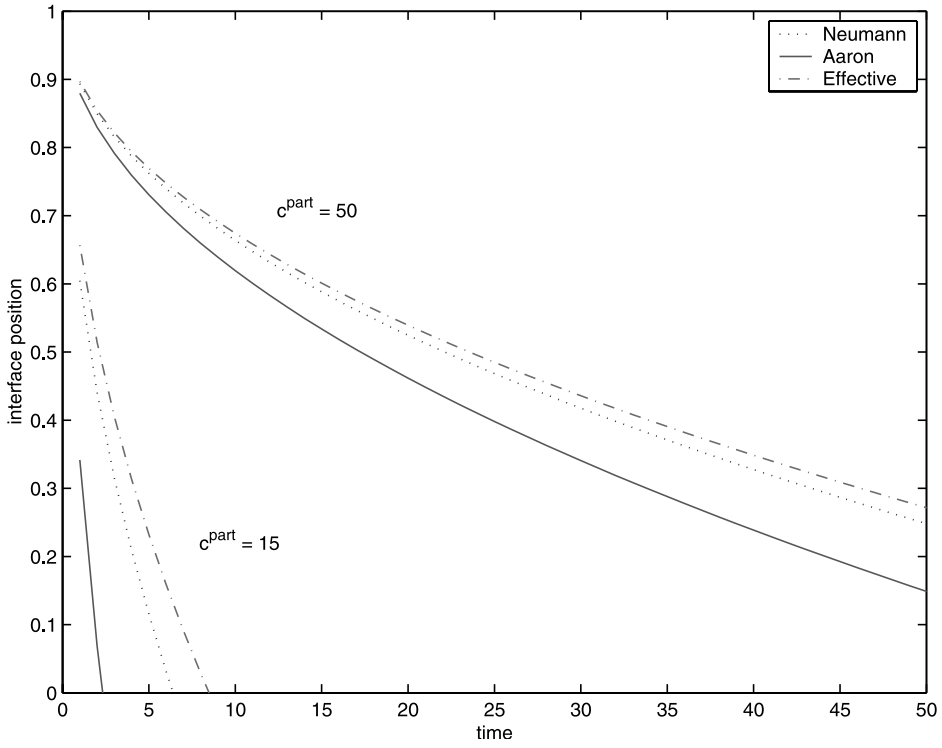

Fig. 3. The interface position as a function of time for the several approaches. The cross-diffusion coefficient $D_{12} = -1$ and the solubility product is $K = 50$. Otherwise the same data set is used as in Fig. 1.

This case is a little more complicated since the particle radius, $S(t)$, is involved in the determination of the interface concentrations. The problem that has to be solved reads as:

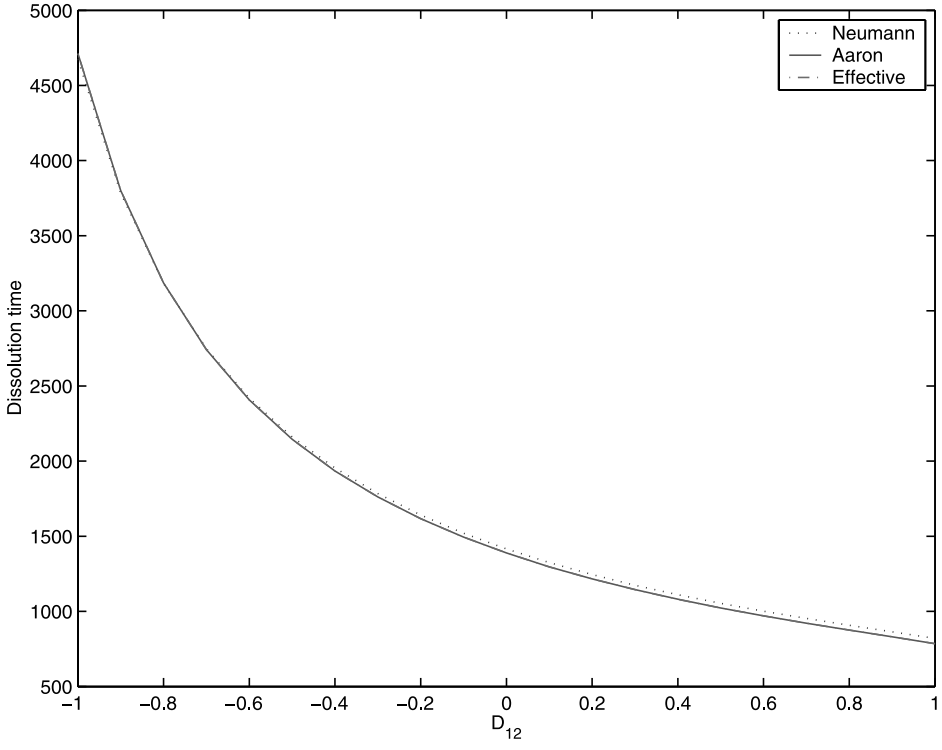

Fig. 4. The dissolution time as a function of the cross-diffusion coefficient D_{12} for the several approaches with otherwise the same data set as in Fig. 1.

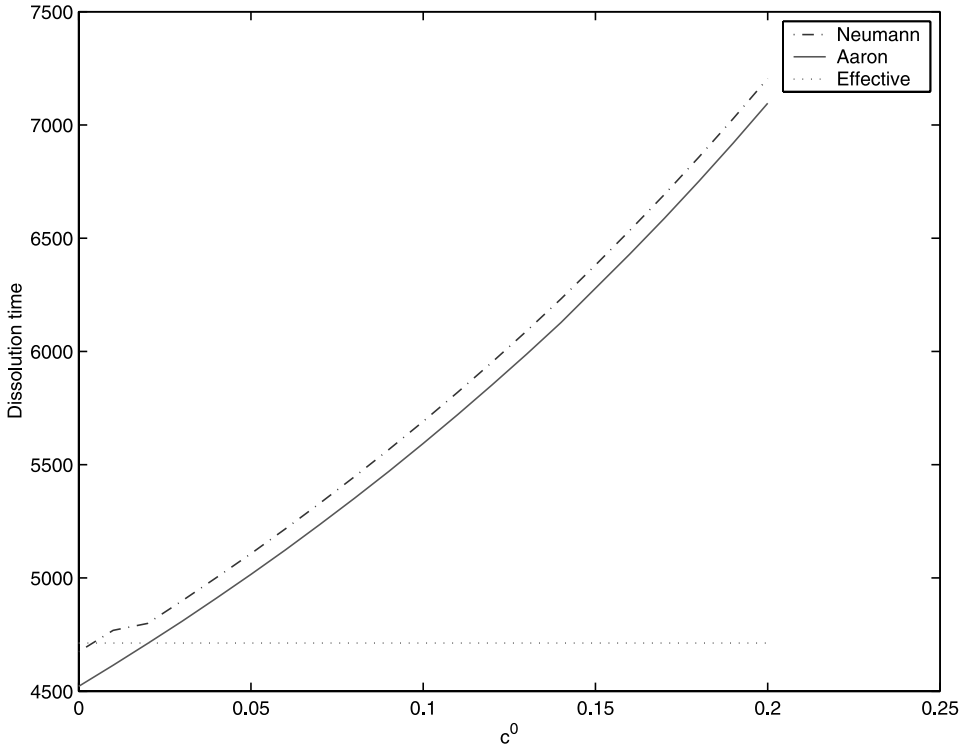

Fig. 5. The dissolution time as a function of the initial concentration $c_i^0 = c^0$ for $D_{12} = -1$ with otherwise the same data as in Fig. 1.

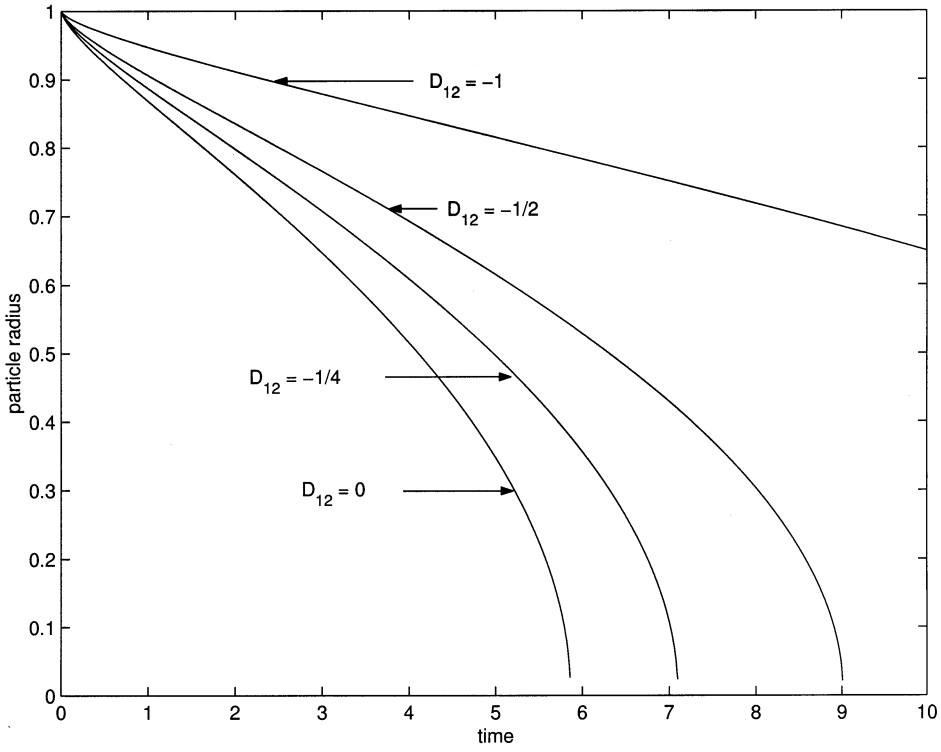

Fig. 6. The interfacial position of a spherical particle as a function of time for the 'Whelan' solution for several values of the cross-diffusion terms. Otherwise the same data set as in Fig. 1 is used.

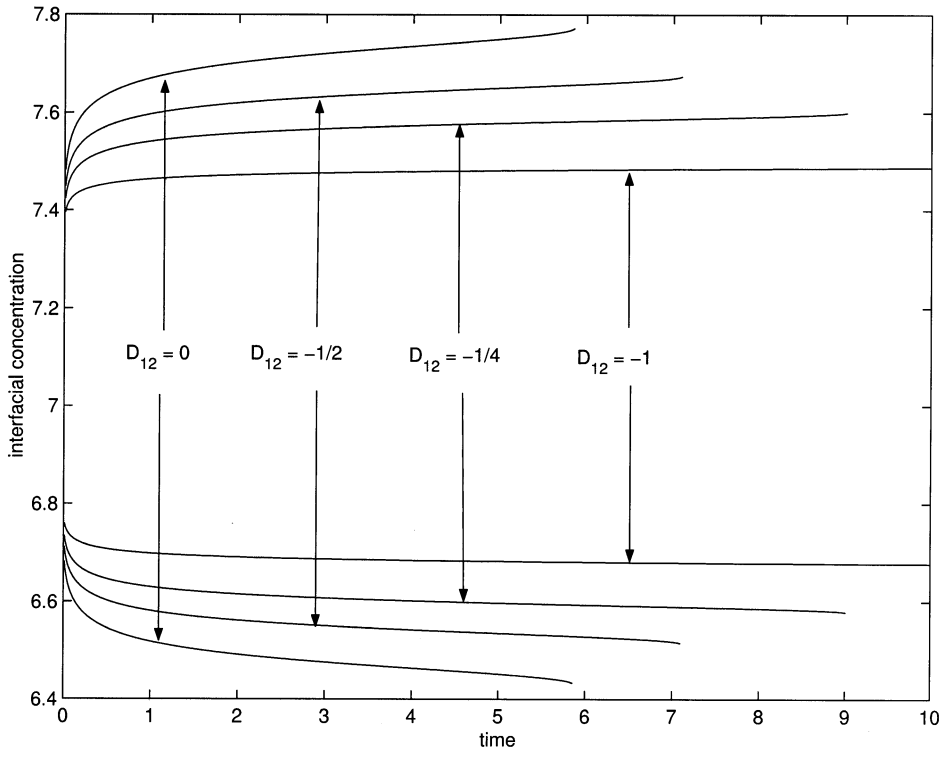

Fig. 7. The interfacial concentrations as a function of time for the 'Whelan' solution for several values of the cross-diffusion terms. Otherwise the same data set as in Fig. 1 is used.

Find $S(t)$ and $\underline{u}^s$ such that

$$\begin{cases} \dfrac{\mathrm{d}S}{\mathrm{d}t} = \dfrac{u_i^0 - u_i^S}{u_i^p - u_i^S}\left(\sqrt{\dfrac{\lambda_i}{\pi t}} + \dfrac{\lambda_i}{S}\right) \\ \left(\displaystyle\sum_{j=1}^{n} P1ju_j^S\right)^{m_1}\left(\sum_{j=1}^{n} P2ju_j^S\right)^{m_2}(\ldots)\left(\sum_{j=1}^{n} P_nju_j^S\right)^{m_n} = K \end{cases} \tag{35}$$

The above problem is solved with the use of combination of a zero-point method to obtain u_i^S combined with a time-integration method to obtain $S(t)$. We show some results in Figs. 6 and 7 where we plot the sphere radius and interface concentrations as a function of time. In constrast to the planar case, it can be seen that the interfacial concentrations do not stay constant. However, we observed that the interface concentrations and interface velocity are equal to the values from the planar case at the very early stages of dissolution (as $t \to 0$). This agrees perfectly with the expectations. Furthermore, a similar effective approach as in Section 4.1 can be derived for the spherical case for sufficiently large t.

5. Numerical experiments

We solved the treated problem for particle dissolution in multi-component alloys with cross-diffusion numerically for a bounded domain. The method is based on Finite Differences combined with a classical moving grid method for the determination of the interface position. Further, the interface concentrations are obtained by an approximate Newton method. The details are described in [15,13].

This section displays some numerical simulations for hypothetical alloys. First we treat an example where the diffusion matrix is diagonalizable and subsequently a non-diagonalizable case is considered.

5.1. The diagonalizable case

As a numerical experiment we show the computation of the dissolution of a planar phase for the case that the diffusion matrix is diagonalizable. Furthermore, we compare the computed numerical solutions with the self-similar solution as developed in Section 4. As input-data we used

$$\begin{aligned} &\underline{c}^0 = (0,\ 0)^{\mathrm{T}}, \qquad \underline{c}^{\mathrm{part}} = (50,\ 50)^{\mathrm{T}}, \\ &D = \begin{pmatrix} 1 & -1/4 \\ -1/4 & 2 \end{pmatrix}, \qquad K = 1. \end{aligned} \tag{36}$$

The above matrix is diagonalizable. In Fig. 8, we plot the interface as a function of time for the (approximate) self-similar solution and the numerical solution. Since $c_i^{\mathrm{part}} \gg c_i^{\mathrm{sol}} > c_i^0 = 0$ we can approximate the solution of (P_1) by the use of Eq. (34). Hence the analytical approaches coincide. At early stages the concentration

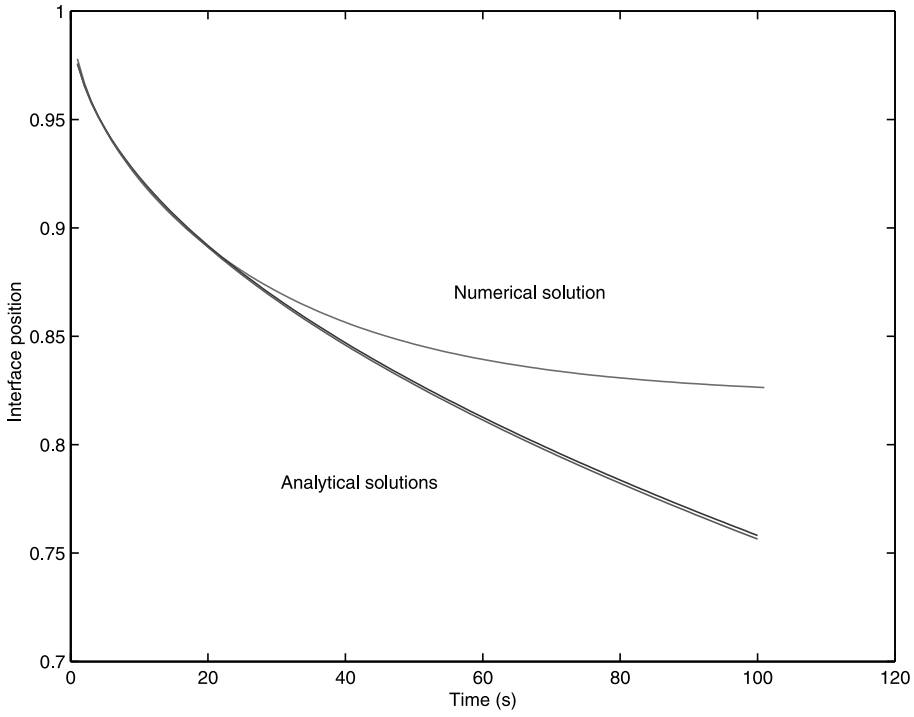

Fig. 8. The interfacial position as a function of time. The dotted curve corresponds to self-similar solution and the solid curve corresponds to the numerical approach.

profiles resemble the profiles that are obtained from the similarity solutions. As time proceeds the dissolution is delayed by soft-impingement at the cell boundary. At this stage, the curve that has been obtained from the numerical computations starts to deviate from the analytical approaches. This effect is clearly visible in

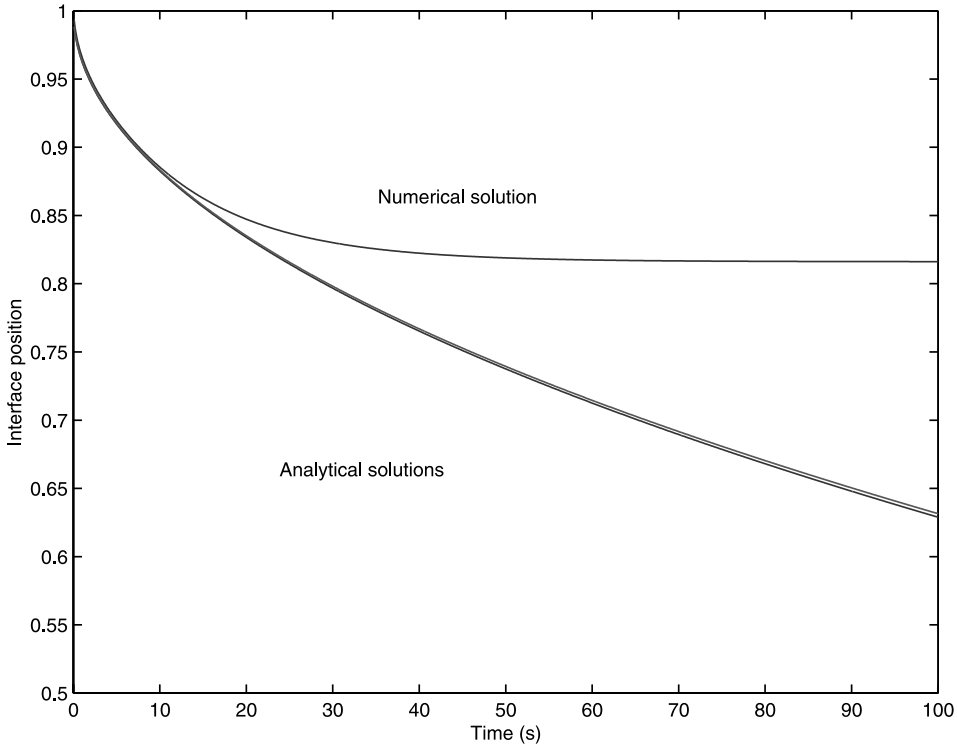

Fig. 9. The interface position as a function of time for the case that the diffusion matrix is not diagonalizable. The analytical and numerical solution are shown.

Fig. 8. From Fig. 8 it is concluded that the numerical scheme is also applicable for cross-diffusion. It can also be seen that the quasi-binary approach is very accurate for this case.

5.2. The non-diagonalizable case

We show results from a computation on a planar particle that dissolves. The diffusion matrix is not diagonalizable for this case. The data-set that we used is given by:

$$\underline{c}^0 = (0,\ 0)^{\mathrm{T}}, \qquad \underline{c}^{\mathrm{part}} = (50,\ 50)^{\mathrm{T}}, \qquad D = \begin{pmatrix} 2 & 1 \\ 0 & 2 \end{pmatrix}, \qquad K = 1. \tag{37}$$

The eigenvalue of the above matrix is equal to 2 and the matrix is not diagonalizable. Further, the numerically computed interfacial position is plotted as the solid line in Fig. 9. We also show the results for the exact solution (see [13]) and the results for the asymptotic approximation (i.e. the quasi-binary approach, see [13]). Similarly as in the preceeding section, we have $c_i^{\mathrm{part}} \gg c_i^{\mathrm{sol}} > c_i^0 = 0$ and hence the exact analytical solution can be approximated by use of the effective concentrations. Hence the analytical approaches co-incide well. Due to soft-impingement at the cell boundary the numerical curve starts to deviate as time proceeds. It can be seen that the curves co-incide well and hence for this case the asymptotic approach is accurate. In Fig. 10, we plot the interface position as a function of time for a particle concentration $\underline{c}^{\mathrm{part}} = (15,\ 15)^{\mathrm{T}}$. Hence now c_i^{part} is not much larger than c_i^{sol} and c_i^0 and hence the asymptotic approximation deviates from the exact Neumann solution, see Fig. 10. The figure illustrates that the asymptotic solution becomes less accurate as c_i^{part} tends to c_i^0. This motivates the restriction to use the asymptotic solution only for cases whenever c_i^{part} is very large compared with the other concentrations in the 'matrix'.

6. Discussion

We extended the models in [14,15] with aspects of cross-diffusion. The developed analytical solutions agree well with solutions obtained from Finite Volume methods. The formalism of the model with cross-diffusion can be found in the book of Kirkaldy and Young [10] or Glicksman [11]. The incorporation of cross-diffusion effects seems necessary from experimental studies of, among others, Kale et al. [7] and from molecular dynamics simulations due to Travis and Gubbins [9]. From our present computations follows that cross-diffusion becomes important when the off-diagonal entries in the diffusion matrix become comparable or larger than the diagonal entries.

The present paper does not contain any characteristics due to the Gibbs–Thomson effect. We remark here

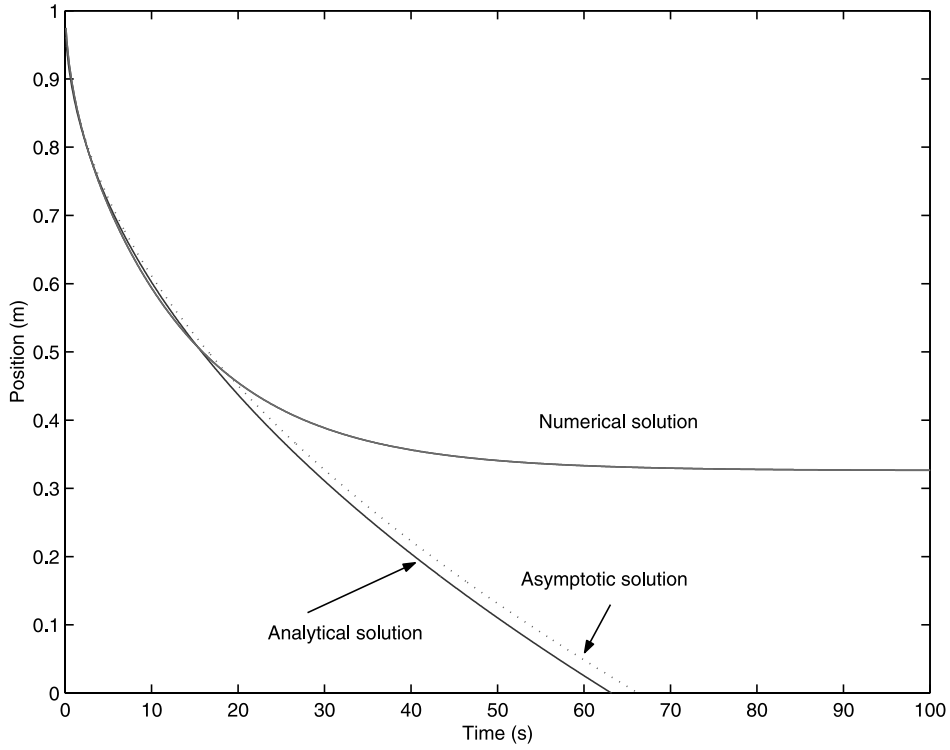

Fig. 10. The interface position as a function of time for the case that the diffusion matrix is not diagonalizable. The analytical and numerical solution is shown. The particle concentrations are $\underline{c}^{\mathrm{part}} = (15,\ 15)^{\mathrm{T}}$.

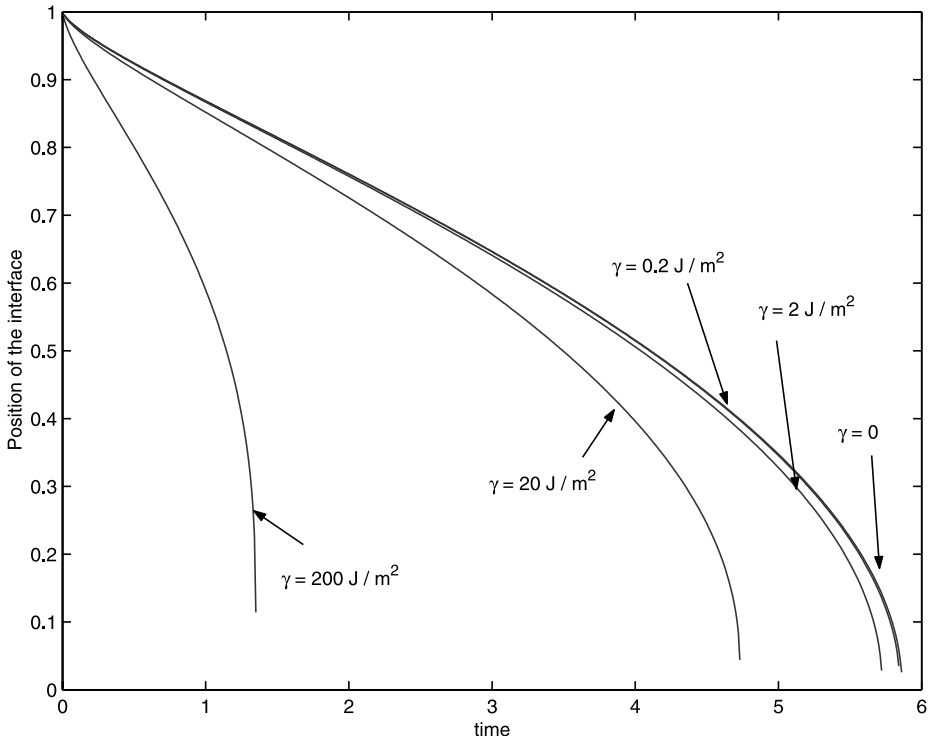

Fig. 11. The interfacial position as a function of time for a spherical particle for several values of the surface tension. The same data set has been used as for Fig. 1 (and Fig. 6) with $D_{12}=0$. In the computations we took $V_m=10^{-5}$ m^3, $R=8.3$ J mol^{-1} K^{-1}, $T=800$ K. Note that the geometry is spherical.

that only dissolution is considered. We note that the case of dissolution of a planar phase gives a stable flat interface where the Gibbs–Thomson effect is not important at all stages of the dissolution process. However, when considering growth, the interface geometry becomes unstable with respect to perturbations, which are present in physical metals as impurities, and fingering starts to occur. We do not comment on this further in the present paper, which covers particle dissolution only.

When considering the dissolution of spherical particles, the Gibbs–Thomson effect enters due to the one-to-one coupling between the interface position and particle curvature. For particles that are initially large, the effect of curvature only comes in at the final stages of the dissolution process. We present some examples in Fig. 11 where we compute the dissolution of spherical particles for different values of the surface tension, where we take the following relation between the solubility product and the interface curvature κ:

$$K=K(\kappa)=K_\infty \exp\left(\frac{2\gamma V_m\kappa}{RT}\right), \tag{38}$$

where κ is the local curvature and V_m, γ, R, T denote the molar volume, surface tension, ideal gas constant and absolute temperature, respectively. From Fig. 11, it can be seen that surface tension effects become important when they are at least in the order of 10 J m^{-2}. Since this value is larger than realistic (which is in the order of 0.2 J m^{-2}), the influence of the surface tension can be disregarded in the computations that were done in the present paper. Note that the curves in Fig. 11 correspond to no cross-diffusion. We plot the interface position as a function of time for the game input, data as in Fig. 11 but now we use $D_{12}=-1=D_{21}$ in Fig. 12. Here the influence due to cross-diffusion is the same as for the case where no surface tension is taken into account. We note that surface tension is important for growth of spherical particles, especially at the initial stages of the growth process.

Of course for a spherical particle follows $\kappa=1/S(t)$ where S is the radius or interface position. The above equation implies that the solubility product increases when the particle radius decreases. This implies that the interfacial (transformed) concentrations can become such that a particle dissolves when the particle radius is small and grows when its radius is large. This effect, Ostwald-ripening, is well-known. Since our model is not able to model 'sub-critical' growth we omit the computation of the growth kinetics of the particle, though later stages of growth can be modeled by the use of the present model.

To deal with cross-diffusion, we present an analytical approach which can be used to determine easily the influence of off-diagonal entries of the diffusion matrix. We present an approach where dissolution times can be

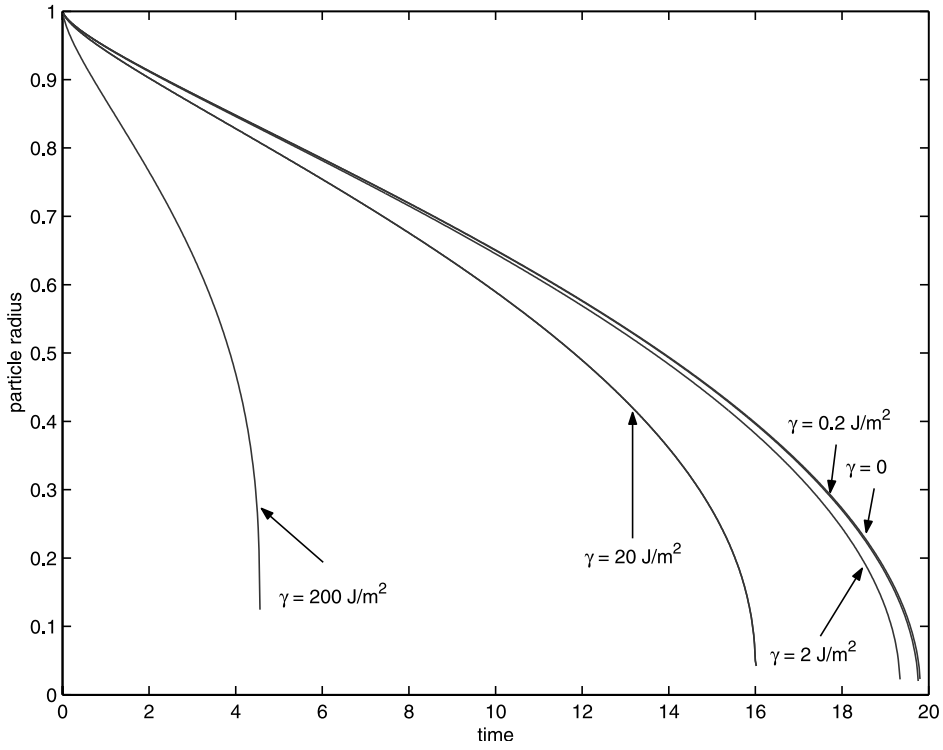

Fig. 12. The interfacial position as a function of time for a spherical particle for several values of the surface tension. The same data set has been used as for Fig. 1 (and Fig. 6) with $D_{12} = -1$. In the computations we took $V_m = 10^{-5}$ m^3, $R = 8.3$ J mol^{-1} K^{-1}, $T = 800$ K. Note that the geometry is spherical.

determined explicitly even without the use of a zero-point method. This approach only holds when the initial concentrations can be disregarded. The numerical Finite Volumes approach is suitable for spherical, cylindrical and planar phases with a finite cell size. This approach is based on the full solution of diffusion equations with moving boundary. Unfortunately, only one spatial coordinate is implemented thus far. Both numerical and analytical solutions are obtained for, respectively, the bounded and unbounded domain. We refer to [13] for the analytical solutions and approximations for the non-diagonalizable case.

The here developed solutions can be used as input for two-dimensional codes to approximate particle dissolution in two spatial dimensions including cross-diffusion effects. However, a full comparison is still lacking.

7. Conclusions

A model, based on a vector-valued Stefan problem, has been developed to predict dissolution kinetics of stoichiometric particles in multi-component alloys. Cross-diffusion of the alloying elements is taken into account, which gives a strong coupling of the differential equations. Using a diagonalization argument, the vector-valued Stefan problem with cross-diffusion is transformed into a vector-valued Stefan problem where the cross-terms vanish whenever the diffusion matrix is diagonalizable. For the diagonalizable case, the numerical solution procedure which is used for modeling particle dissolution/growth when no cross-diffusion is taken into account, can be used. Well-known mathematical implications, concerning mass-conservation of the Stefan problem and self-similarity solutions can be recovered now also for the case of cross-diffusion. The hyperbolic relation between the interfacial concentrations becomes more complicated, however, since the eigenvectors of the diffusion matrix have to be taken into account as well. In spite of this complication, the vector-valued Stefan problem can be approximated by a quasi-binary problem in a similar way as for the case in which no cross-diffusion is taken into account. The advantages of the diagonalization procedure are.

(i) The eigenvalues give a quick insight into the well-posedness of the problem, negative eigenvalues are not allowed. Existence of solutions for singular diffusion matrices has been analyzed in [13].

(ii) For the numerical computations the concentration profiles can easily be computed using fully implicit methods similarly to the case of multi-component diffusion without cross-diffusion terms.

Similar as in the case of no cross-diffusion we obtain expressions for the quasi-binary approach.

References

[1] M.J. Whelan, Metals Science Journal 3 (1969) 95–97.
[2] F.V. Nolfi, Jr, P.G. Shewmon, J.S. Foster, Transactions of the Metallurgical Society of AIME 245 (1969) 1427–1433.
[3] O. Rciso, N. Ryum, J. Strid, Metallurgical Transactions A 24A (1993) 2629–2641.
[4] R. Hubcrt, ATB Metallurgie 34–35 (1995) 4–14.
[5] R. Kobayashi, Physics D 63 (1993) 410–423.
[6] U. Grafe, B. Bottger, J. Tiadcn, S.G. Fries, Scripta Materialia 42 (12) (2000) 1179–1186.
[7] G.B. Kalc, K. Bhanumurthy, S.K. Khera, M.K. Asundi, Materials Transactions 32 (11) (1991) 1034–1041.
[8] A. Vergara, L. Paduano, V. Vitagliano, R. Sartorio, Materials Chemistry and Physics 66 (2000) 126–131.
[9] K.P. Travis, K.E. Gubbins, Molecular Simulation 27 (5–6) (2001) 405–439.
[10] J.S. Kirkaldy, D.J. Young, Diffusion in the Condensed State, The Institute of Metals, London, 1987.
[11] M.E. Glicksman, Diffusion in Solids, Wiley, New York, 2000.
[12] E.B. Naumann, J. Savoca, AICHE Journal 47 (5) (2001) 1016–1021.
[13] F.J. Vermolen, C. Vuik, S. van der Zwaag, Some mathematical aspects of particle dissolution and cross-diffusion in multi-component alloys, Delft University of Technology, 001, Department of Applied Mathematical Analysis, see http://ta.twi.tudelft.nl/TWA-Reports/01-15.ps, 01-13, Delft, The Netherlands.
[14] F.J. Vermolen, C. Vuik, Journal of Computational and Applied Mathematics 93 (1998) 123–143.
[15] F.J. Vermolen, C. Vuik, Journal of Computational and Applied Mathematics 126 (2001) 233–254.
[16] F.J. Vermolen, C. Vuik, S. van der Zwaag, Materials Science and Engineering A328 (2002) 14–25.
[17] M. Farkas, Nonlinear Analysis, Theory, Methods and Applications 30 (1997) 1225–1233.
[18] J. Crank, Free and Moving Boundary Problems, Clarendon Press, Oxford, 1984.
[19] J. Chadam, H. Rasmusscn, Free Boundary Problems Involving Solids, Longman, Scientific and Technical Harlow, 1993.
[20] A. Visintin, Models of Phase Transitions, Progress in Nonlinear Differential Equations and their Application, vol. 38, Birkhauser, Boston, 1996.
[21] G.H. Golub, C.P. van Loan, Matrix Computations, third ed., The Johns Hopkins University Press, Baltimore, 1996.
[22] J.S. Kirkaldy, D. Weichert, Z.-U. Haq, Canadian Journal of Physics 41 (1963) 2166–2173.
[23] H.B. Aaron, G.R. Kotler, Metallurgical Transactions 2 (1971) 1651–1656.